Volume 4, Number 1 (March, 2011) p. 001 - 030 • ISSN 1983-4195

IBRACON

REVISTA IBRACON DE ESTRUTURAS E MATERIAIS

IBRACON STRUCTURES AND MATERIALS JOURNAL

Influence of steel fibers on structural behavior of beams strengthened with CFRP

Influência de fibras de aço no comportamento estrutural de vigotas reforçadas com PRFC

V. J. FERRARI [a]
vladimirjf@hotmail.com

J. B. DE HANAI [b]
jbhanai@sc.usp.br

Abstract

In this study we present the methodology and the results from the analysis of behavior of reinforced beams and externally strengthened until the flexural with sheet of CFRP (carbon fiber reinforced polymer).The strengthening behavior of common concrete beams is analyzed and compared with the strengthening of beams molded with mortar cement composite and short steel fibers. The main objective was to investigate the influence of cement composite (chosen without major criteria) on the behavior and failure mode of the strengthened beams. Flexural tests in three points of six beams and characterization tests of materials (flexural tests in three points in engraved prismatic bodies-of-proof, strain tests in steel bars and axial compression tests in cylindrical bodies-of-proof) were carried out. In addition, a finite element analysis has been performed to compare to experimental results. The increase of toughness and crack strength lead to significant changes in the structural behavior of beams with fibers and strengthened when compared to strengthened common concrete beams.

Keywords: cement composite; strengthened beams; bending; toughness.

Resumo

Neste trabalho, apresenta-se a metodologia utilizada e os resultados da análise do comportamento de vigotas armadas e reforçadas externamente à flexão com manta de PRFC (polímeros reforçados com fibras de carbono). Avalia-se o comportamento do reforço de vigotas de concreto comum e compara-o com o do reforço de vigotas moldadas com um compósito cimentício à base de argamassa e fibras curtas de aço. O objetivo principal foi investigar a influência do compósito cimentício (escolhido sem maiores critérios) sobre o comportamento e o modo de ruína das vigotas reforçadas. Para tanto, uma série de ensaios de flexão em três pontos em seis vigotas foi conduzida, além dos ensaios de caracterização dos materiais: ensaios de flexão em três pontos em corpos-de-prova prismáticos entalhados, ensaios de tração em barras de aço e ensaios de compressão axial em corpos-de-prova cilíndricos. Adicionalmente, uma análise de elementos finitos foi desenvolvida com objetivo de comparar os resultados obtidos com os experimentais. O ganho de tenacidade e de resistência à fissuração provocou mudanças significativas no desempenho da vigota moldada com fibras e reforçada quando comparada com a vigota reforçada de concreto comum.

Palavras-chave: compósito cimentício, vigotas reforçadas, flexão, tenacidade.

[a] *Universidade Estadual de Maringá, Departamento de Engenharia Agrícola, vladimirjf@hotmail.com, Rodovia PR-182, Cidade Gaúcha-PR, Brasil;*
[b] *Universidade de São Paulo, Departamento de Estruturas, Escola de Engenharia de São Carlos, jbhanai@sc.usp.br, São Carlos, Brasil.*

Received: 23 Apr 2010 • Accepted: 25 Oct 2010 • Available Online: 04 Mar 2011

Figure 1 – Strengthened beam failure by debonding (Ferrari (1))

Figure 2 – Cement matrices behavior (Ferrari (1))

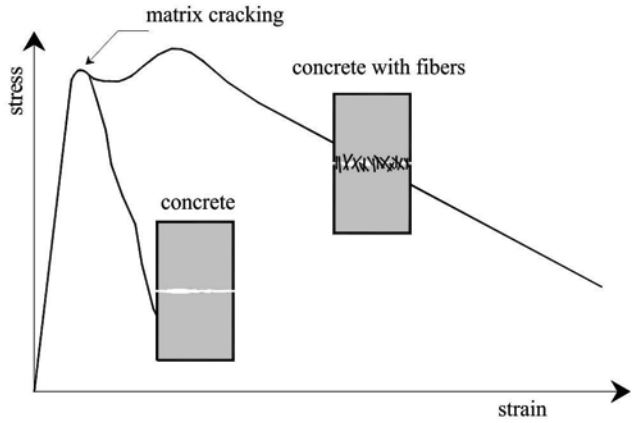

1. Introduction

The use of CFRP (carbon fiber reinforced polymers) has been continuously increased in cases of structural strengthening throughout the world in the last decade. However, its use from the standpoint of structural mechanics, presents an inconvenient related to its efficacy and security, which is its fragile and premature debonding in reinforce-concrete linkage region. Such failure, if not considered in the project, can decrease the efficacy of strengthening significantly (Ferrari [1], Buyukozturk [2], Wu [3]).

As shown in Ferrari [1], the strengthening debonding, generally, originates from regions where exist concentration of high stresses, as the discontinuity of material (strengthening extremity) and the presence of cracks (Figure [1]). According to Buyukozturk [2], the major failures by debonding reported in literature, originates on substrate of concrete.

On the other hand, is known that the incorporation of short steel fibers (with high strength and ductility) on cement matrix of concrete can improve its load and deformation capacity. The presences of these fibers can not improve the matrix strength, however, maintain a load of capacity post-cracking and supports deformations larger than the single matrix, as shown in Figure [2].

In This way, this study investigates the influence of a cement composite mortar and short steel fibers-based on the behavior and failure mode of strengthened beams. For this purpose, we present the methodology and results from the behavior analysis of reinforced beams and externally strengthened until the flexural with sheet of CFRP. The strengthening behavior from beams of common concrete is assessed and compared to the strengthening of beams molded with the cement composite.

We expect that the gain of toughness and strength in front of the ad-

Table 1 – Nomenclature and characteristics of beams

Group	Beams	Characteristics	Age (days)	
			Strengthening	Test
A	VRE-1 VRE-2	Concrete beams without external strengthening. Reference to comparison with to other groups.	-	25
B	VR1-1 VR1-2	Concrete beams with external strengthening in its lower flangeformed by a sheet layer of CFRP.	7	25
C	VR2-1 VR2-2	Molded beams with mortar cement composite with addition of short steel fibers. External strengthening with a sheet layer of CFRP.	7	26

vance of cracks provided by the cement composite can lead to significant changes in the structural performance of strengthening when compared to strengthened beams molded with common concrete.

2. Experimental Program

2.1 Test configuration and instrumentation

The beams dimensions and the general test aspects are shown in Figure [3]. Were analyzed six reinforced beams with dimensions of 15 cm x 15 cm x 75 cm and a free span of 65 cm, which were distributed into three groups according to Table [1].
The longitudinal reinforcement of beams, inferior and superior, was constituted by two steel bars CA-60 of 6,0 mm diameter, corresponding at a reinforcement rate of r=0,25%. This reinforcement was dimensioned in Domain 2 of deformation. The transverse reinforcement, constituted by steel wires CA-60 of 5,0 mm spaced of 8 cm, was dimensioned to prevent the beam failure by shearing.
The tests were performed at Laboratório de Estruturas da Escola de Engenharia de São Carlos (LE-EESC), using a servo-hydraulic equipment of Instron mark model 8506, which allowed to apply the loading by the control of piston displacement at a rate of 0,005 mm/s.
During the tests accomplishment, was conducted the monitoring of strength, displacements and specific deformations using an automatic system of data acquirement. The measurement of vertical displacements in the midspan was obtained using a transducer of displacements which was lean on a “yoke” sup-

Figure 3 – Beams dimensions and general aspect of the test

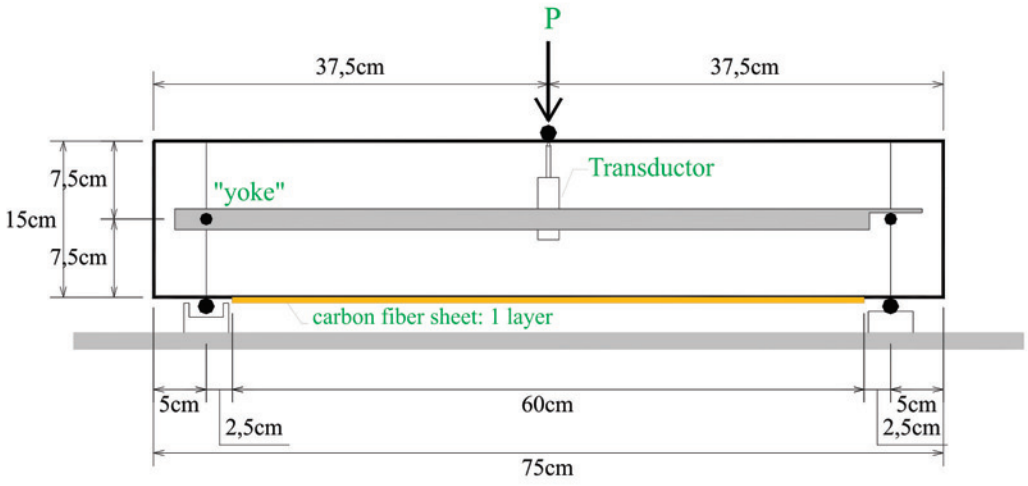

a) Beams dimensions

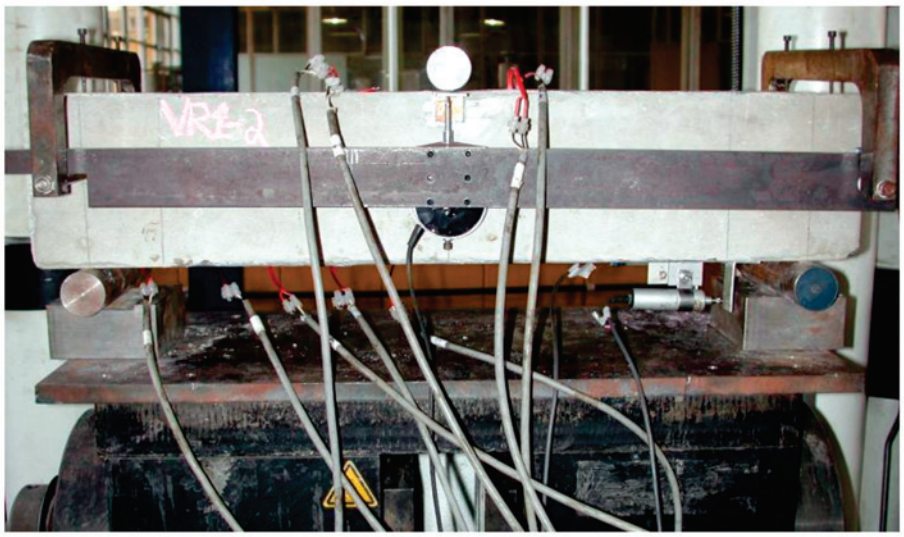

b) General aspect of flexural test in three points

Figure 4 – Strain gauges arrangement in the strengthening

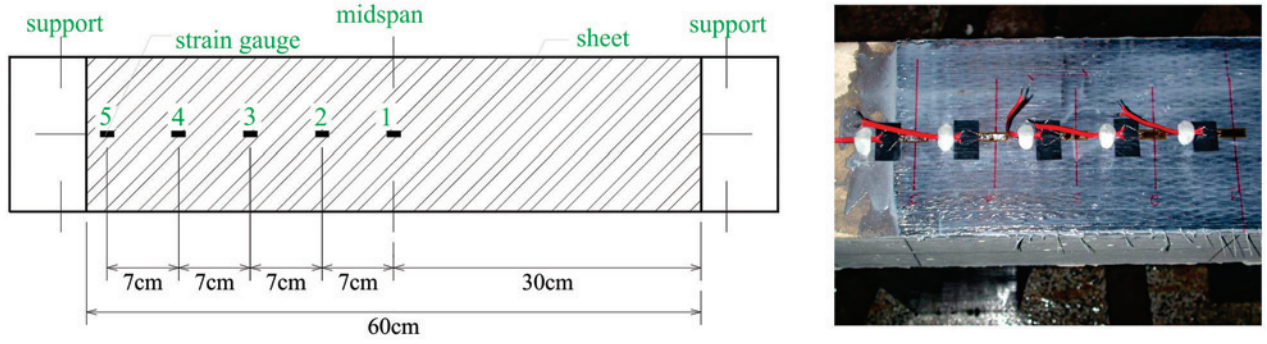

a) strain gauges arrangement

b) attached strain gauges

port. Electric extensometers of strength (*strain gauges*) were attached to concrete, reinforcement and along the strengthening to obtain deformation values. Both the reinforcement steel bars and compressed region of concrete were implemented in the central section of beam. While the extensometers arrangement on the strengthening is illustrated in Figure [4].

The group A was represented by two beams of reinforced concrete without external strengthening and named VRE. These are beams of reference to make comparison to others. The group B was represented by other two beams, named VR1, of reinforced concrete strengthened in its lower flange by the attachment of a sheet layer of CFRP. While group C was represented by two strengthened beams named VR2. These beams were molded using a cement composite of mortar with the addition of short steel fibers. The idea of cement composite is to confer to beams of these group better conditions of strength to propagation of cracks intending to reach a better strengthening performance.

2.2 Beams molding and strengthening attachment

For beams molding of the groups A and B was produced a conventional concrete without the incorporation of additive. While beams of group C were molded with the production of a cement composite with addition of short steel fibers. The used compositions are described in Table [2]. For characterization of concrete and mortar composite were molded for each beam, five cylindrical specimens of 10x20 cm and three prismatic specimens of 15x15x50 cm.

The strengthening with carbon-fiber sheet was applied on strained flange of beams following the subsequent technical procedures:

- Removal of a very thin superficial layer of cement cream until the partial exposure of aggregates;
- The sheet cut in needed dimensions and mixture of epoxy and thixotropic bi-component adhesive in a proportion of mass following the manufacturer suggestions;
- Application of a thin adhesive layer along the beam substrate

Table 2 – Composition of materials mixture for beams molding

Material	Concrete		Composite	
	Mass trace	Specific mass	Mass trace	Specific mass
Cement CP-V ARI PLUS	1,0	3,15 kg/dm^3	1,0	3,15 kg/dm^3
Sand	2,3	2,65 kg/dm^3	3,0	2,65 kg/dm^3
Aggregate 1	2,3	2,70 kg/dm^3	-	-
a/c	0,5	-	0,5	-
Cement consumption (kg/m^3)	400	-	512	-
Steel fiber*	-	-	2%	7,80 kg/dm^3
Aditive – Glênium 51	-	-	0,4%	1,09 kg/dm^3

*short steel fiber with 25mm length and 0,75mm diameter

Table 3 – Properties of strengthening system

Properties	Carbon fibers*	Epoxy resin**
Effective thickness	0,17mm	-
Tensile strength	2.603 MPa	30 MPa
Elasticity module	209.000 MPa	3.800 MPa
Ultimate deformation	13‰	9‰
Mixture proportion	-	4:1 em massa
Consumption	-	0,7 a 1,2 kg/m^2

* in conformity with the conducted characterization by Carrazedo (4);
** in conformity with manufacturer suggestions

Table 4 – Results of compression tests

Group	f_{cm} (MPa)	$f_{ctm,sp}$ (MPa)	E_{cs} (MPa)
A	49,86	3,90	32.403
B	49,86	3,90	32.403
C	43,11	3,95	24.955

f_{cm}: average strength under concrete compression;
$f_{ctm,sp}$: average strength under indirect tensile on concrete;
E_{cs}: secant-module of deformation;

with a help from a metallic spatula;

- The sheet placement above the adhesive, pressing it with the own hands and then with a little metallic roll, forcing the adhesive reflow among the carbon fibers.

The mechanical properties of the carbon-fiber sheet and the epoxy resin are indicated in Table [3].

3. Materials characterization

3.1. Tests of compression on cylindrical specimens

The cylindrical specimens were submitted to axial compression tests – NBR 5739 [5] – and strain tests by diametric compression – NBR 7222 [6] – on the same date in which each correspondent beams were tested. The mean values of individual results are presented in Table [4].
In Figure [5] are presented stress-strain curves obtained for concrete and cement composite.

3.2. Tests of tensile on steel bars

Were tested three samples of steel bars in according to established suggestions in NBRISO 6892 [7]. The results are presented in Table [5] and in Figure [6] is illustrated the test accomplishment and the obtained stress-strain diagram.

Figure 5 – Stress-strain curves of composite and common concrete

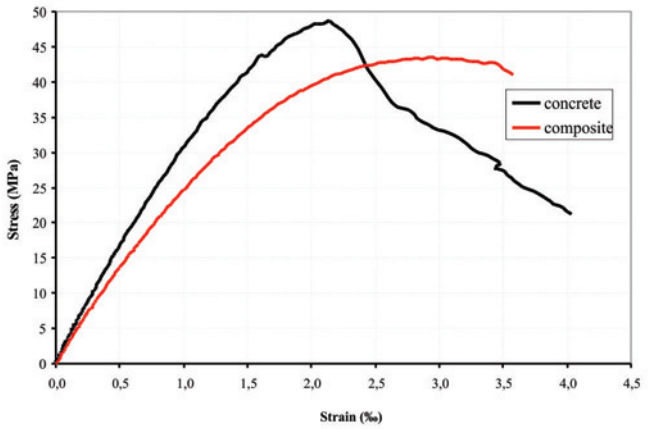

3.3. Flexural tests in notched specimens

To evaluate the stress behavior in the concrete flexural and the fibers and mortar-cement composite were conducted flexural tests in three points of notched prismatic specimens. It was followed the RILEM TC 162-TDF [8] suggestions to the tests conduction.
In Figure [7] are showed the P-CMOD (*crack mouth opening displacement*) "mean" curves, representative of materials behavior on flexural and in the Table [6] results are presented.
Despite of concrete possessing higher strength than the mortar composite, loses its load capacity almost immediately after reach maximum strength. While the mortar composite maintains its capacity resistant even after the matrix cracking. This characteristic may be fundamental to provide better performance to the strengthening after the material cracking which constitute the strained flange of the beam.

Table 5 – Results of tensile test in steel bars

Sample	f_y (MPa)	e_y* (‰)	e_y (‰)	E_s (MPa)	f_{st} (MPa)
1 5 mm	629,54	3,12	5,05	198.392	672,27
2 5 mm	637,28	3,02	4,86	190.614	672,27
Mean	633,41	3,07	4,96	194.503	672,27
1 6 mm	658,43	3,01	5,12	205.799	-
2 6 mm	660,87	2,88	4,90	210.578	822,42
3 6 mm	656,00	-	-	-	844,46
Mean	658,43	2,95	5,01	208.189	833,44

ε_y* hardening deformation correspondent to the bilineardiagram.

Based on the P-CMOD response of materials, was verified an almost fragile behavior for concrete, whereas the cement composite showed a pseudo strain-hardening characteristic. The increases in equivalent and residual values of flexional strength, in relation to the f_{fctL} stress, indicate increase in flexional toughness of this material due to the contribution of steel fibers.

The obtained fracture energy for concrete was 154,92 N/m, calculated in according to RILEM [9]. This value is higher than the theorically estimated (103,87 N/m) by the eq. [1], suggested by the model code FIB [10].

for $f_{cm} \leq 80$ MPa [1]

$$G_F = G_{F0}\left(\frac{f_{cm}}{f_{cm0}}\right)^{0,7}$$

Where G_{F0} estimated as function of maximum diameter of large agregates ($d_{máx}$) by Box 1, and f_{cm0} = 10 MPa.

4. Presentation and results analysis

4.1. Observed failure modes

The reinforced concrete beams without strengthening presented expected and compatible failure mode with the dimensioning, that is, excessive deformation of inferior longitudinal reinforcement without the crushing of compressed concrete. The test was suspended when the reinforcement deformation was approximately 15,7‰. At this time, beams showed few cracks of large openings propagated along practically all its height.

Among the strengthened beams of group B and C, different failure modes were obtained. For the strengthened beams of group B

Figure 6 – Steel bars characterization

a) tensile test

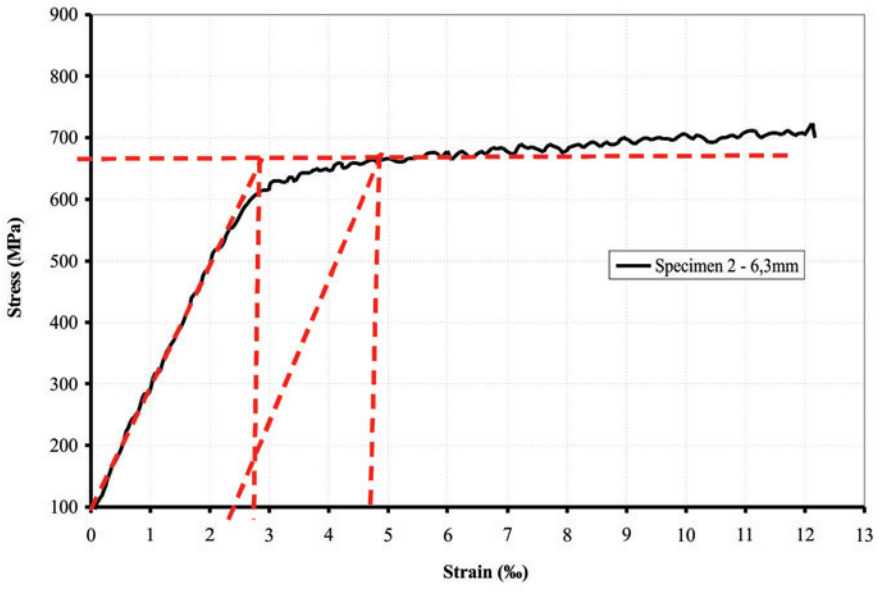

b) stress-strain curve

Box 4.1 – G_{F0} values in accord to FIB (9)

d_{max} (mm)	8	16	32
G_{f0} (N/mm)	0,02	0,03	0,05

Figure 7 – Mean P-CMOD curves for the concrete and composite

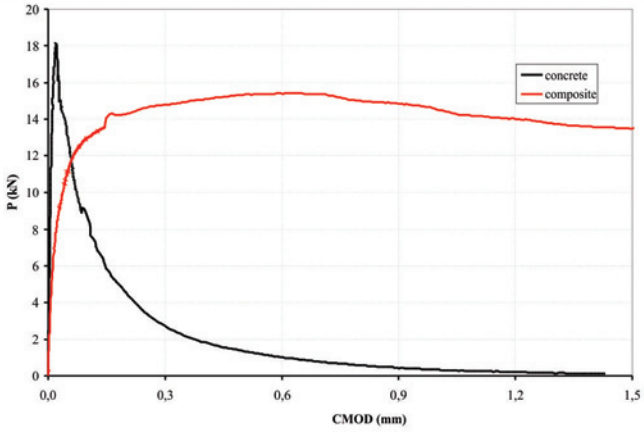

(VR1-1 e VR1-2) molded with common concrete, failure was given by separation of a concrete piece from the reinforcement cover layer, followed by the strengthening release practically from the shearing midspan (Figure [8]).

For the strengthened beams of group C, the failure mode was characterized by extracting the cover layer from the longitudinal inferior reinforcement. The failure initiated at strengthening end appearing a crack which propagated slowly (steel fibers action) and in an inclined manner until the reinforcement. This crack advanced horizontally, on the reinforcement level, and led to the cover layer separation (Figure [9]).

It is important to consider that for beams of group C, the mode and position to failure were altered from partial separation in the shearing midspan to the extraction of the cover layer at the strengthening end. This change reflects the elimination of strengthening release, as observed for beams of group B, due to the effects of steel fibers presence in cement-mortar composite.

4.2. Loads

The influence of cement composite on the strengthened beams behavior can be evaluated through the loads analysis indicated in Table [7] and with the established comparisons in Figure [10]. The crack load (P_f) corresponds to the load in which is observed accentuated inclination change of P-d curve in its ascendant branch. The load correspondent to the longitudinal reinforcement yield (P_y) was obtained when the mean deformation of beam steel bars were equivalent to the deformation value of yield e_y^* obtained from tensile tests of steel bars. The ultimate load (P_u) corresponds to the value of failure load of beam.

As expected, strengthened beams of common concrete presented cracking load, reinforcement yield and failure values higher than the beams without strengthening. The verified average increases were, respectively, of the order of 22%, 110% and 56%. These increases are still more significant when compared with the average loads obtained for beams of group C. In this case the verified increases in relation to beams without strengthening were of 8%, 112%, and 116%.

The average cracking load of beams of group C was inferior to the group B, therefore in accordance with the conducted characterization, the concrete possess higher tensile strength in flexural than the

Table 6 – Strengths and stress in accord to RILEM (8)

Material	Strengths (kN)						Stress (MPa)					
	F_L		F_M		$F_{R,1}$		$f_{fct,L}$		$f_{eq,2}$		$f_{R,1}$	
Concrete	14,67 17,79 18,14	16,87	14,67 17,79 18,14	16,87	1,80 - 0,86	1,33	4,22 5,12 5,22	4,85		-	0,52 - 0,25	0,39
Composite	11,94 ~~18,42~~ 13,37	12,66	12,83 ~~20,94~~ 15,41	14,12	12,82 ~~20,87~~ 15,36	14,09	3,40 ~~5,29~~ 3,97	3,69	3,66 ~~5,98~~ 4,59	4,13	3,61 ~~5,99~~ 4,56	4,09

F_L – maximum strength of offset;
F_M – maximum strength supported by material;
$F_{R,1}$ – correspondent strength to vertical displacement of 0,46mm;
$f_{fct,L}$ – correspondent stress to a strength FL;
$f_{eq,2}$ – equivalent stress to flexural tensile;
$f_{R,1}$ – residual stress;

Figure 8 – Failure in strengthened beams of group B

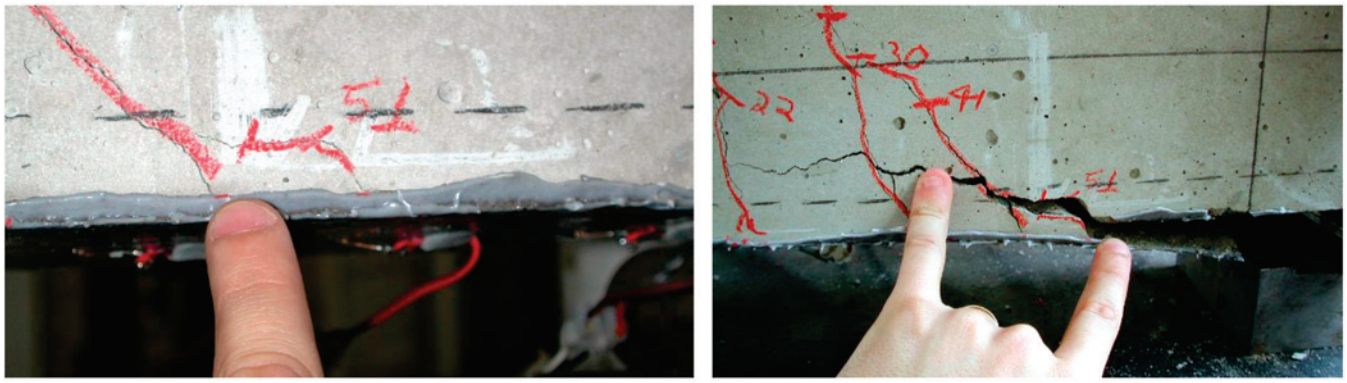

a) crack formation

b) crack propagation after debonding

Figure (9) – Failure in strengthened beams of group C

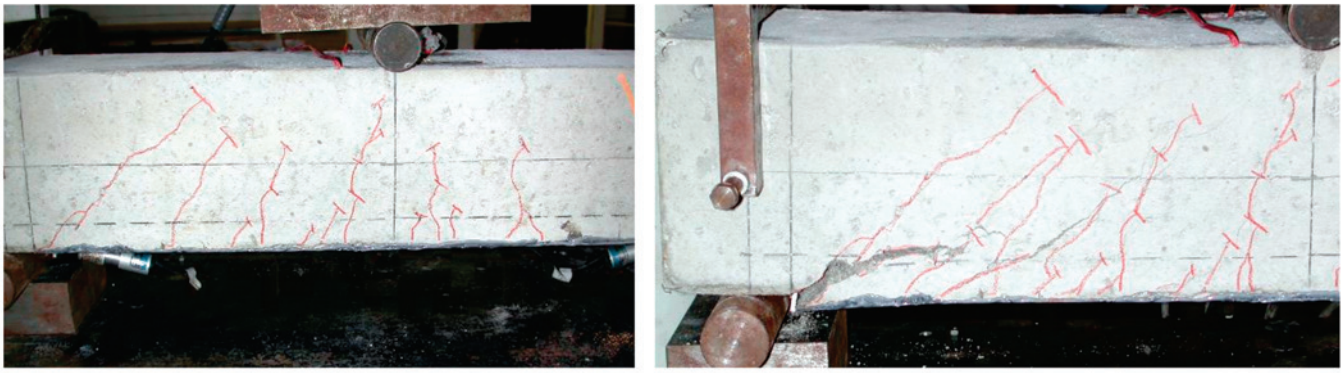

a) main crack in the strengthening end

b) crack propagation

Table 7 – Loads and modes of failure observed

Group	Beams	P_f (kN)		P_y (kN)		P_u (kN)		Modes of failure
A	VRE-1 VRE-2	14,18 13,84	14,01	26,17 21,68	23,93	40,25 36,45	38,35	Excessive deformation of the inferior reinforcement
B	VR1-1 VR1-2	17,42 16,90	17,16	48,84 51,66	50,25	61,93 57,81	59,87	Concrete layer partial separation and strengthening debonding
C	VR2-1 VR2-2	14,75 15,50	15,13	53,21 53,27	53,24	79,67 86,21	82,94	Cover layer extracting

Figure 10 – Comparison among loads

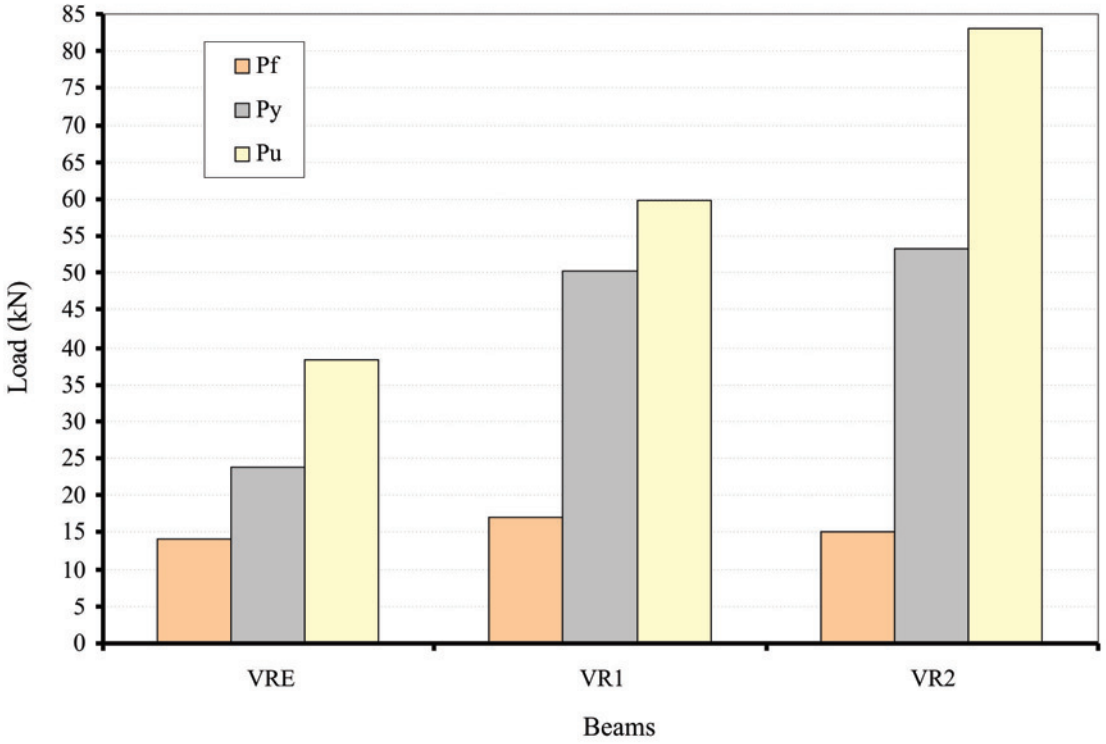

Figure 11 – Curve P-δ in the midspan

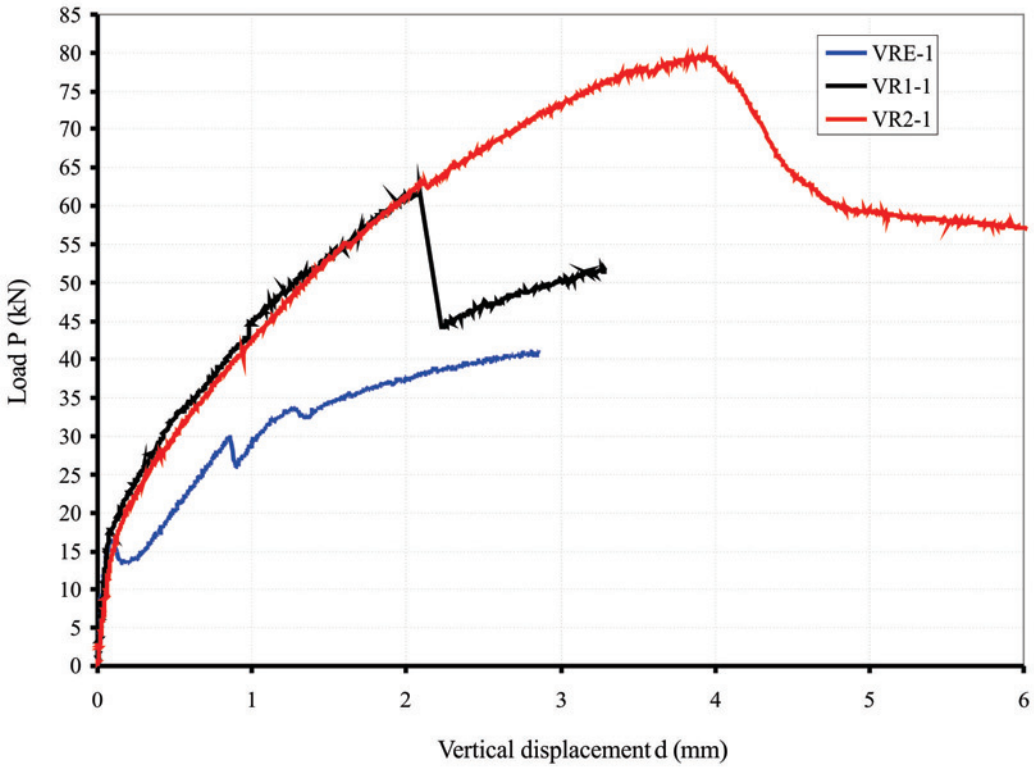

mortar-cement composite. Until appearing the first crack is the concrete situated below the neutral line that resists the normal stress of tensile. Soon, the concrete beam cracked in a higher level of loading. The beams of group C comparatively to the strengthened of concrete, presented higher values of failure and yield load. The verified increases were respectively 6% and 39%. Showing that the steel fibers exerted influences on yield load of reinforcement and mainly, on the rupture load of strengthened beam.

4.3. Vertical displacements

The Figure [11] congregates curves experimentally obtained of vertical load-displacement in the midspan (P-δ) for strengthened beams and without strengthening. With the intention of a better visualization, only the behavior of a single beam of each group is presented. It is also important to mention that among beams of each group their behaviors were similar.

The presence of strengthening in reinforced concrete beam (VR1-1) provided increase in load capacity and, after cracking of concrete, gains in the section stiffness.

The P-d curve of VR2-1 beam shows a high deformation and load capacity before the rupture. The descending branch of the curve presents a softer fall, which reflects a more ductile failure proportioned by steel fibers.

The addition of steel fibers substantially improved the post-cracking behavior and the ductility of strengthened beam VR2-1. Whereas, the failure of beam VR1-1 occurred in a fragile mode due to the debonding of strengthening. Consequently, the loss of gradual strength verified in the beam VR2-1 is an important evidence that can be considered as a favorable aspect in the structural behavior.

Figure 12 – Reinforcement strains and in strengthening in the midspan of beams

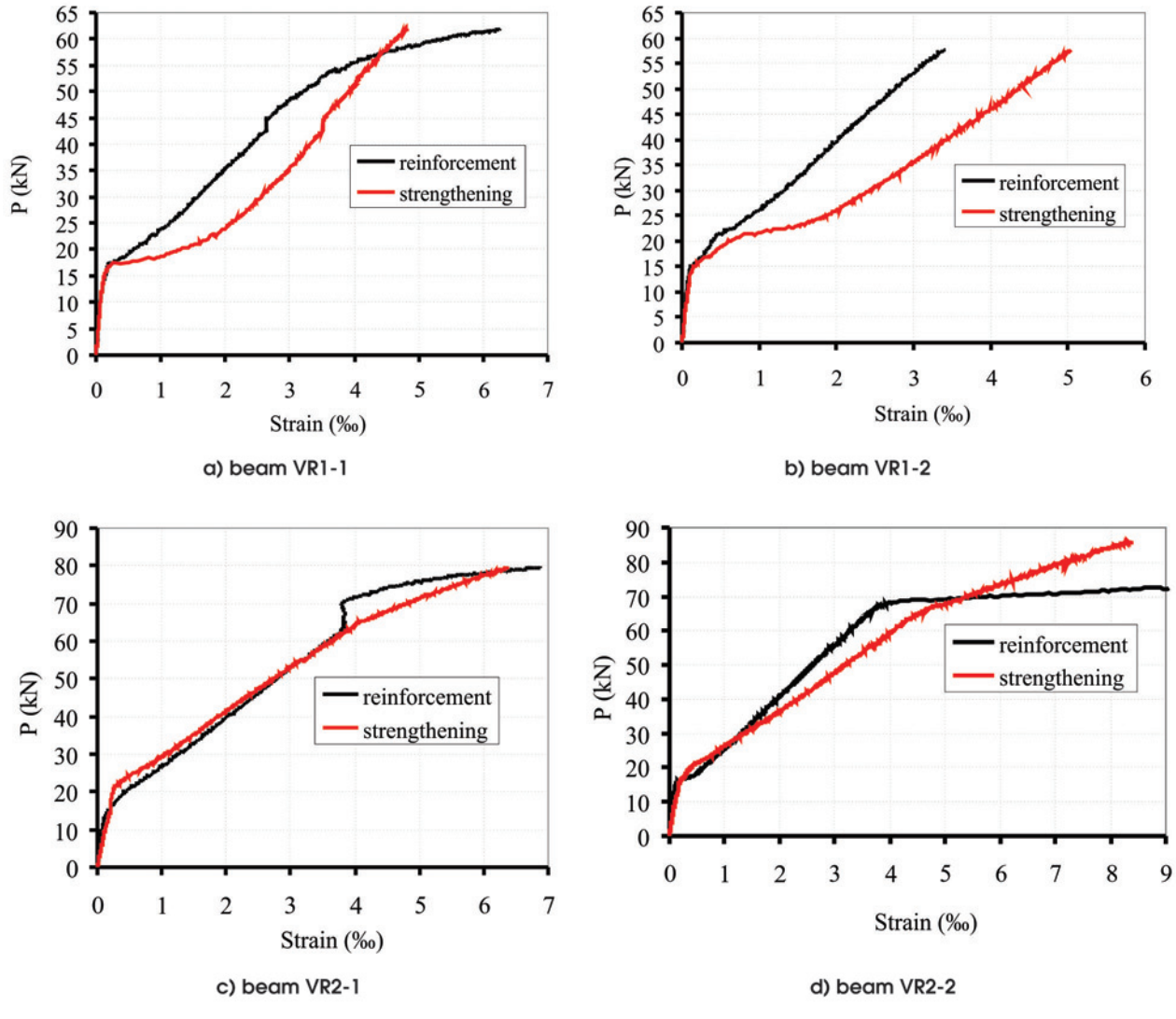

Figure 13 – Comparison among strains in the strengthening of beams

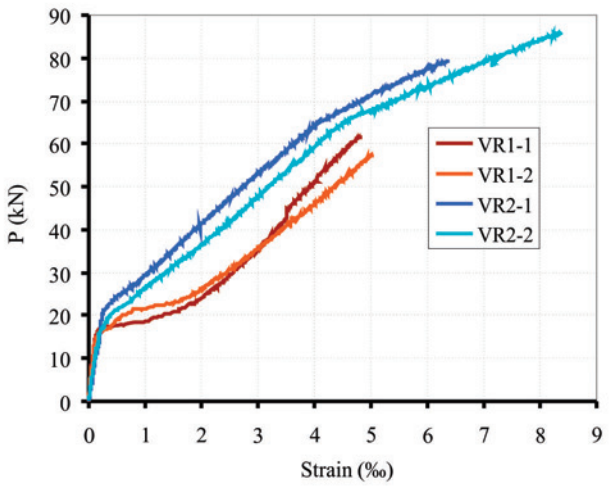

a) strain in the midspan

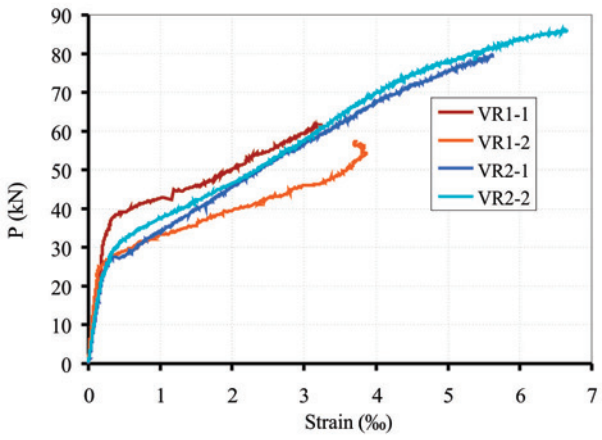

b) strain in the shearing midspan

4.4. Strains

In Figure [12] are congregated the strength-deformation diagrams specific of reinforcement and strengthening in the midspan for beams of group B and C. From the diagrams analysis, is possible to do some commentaries as the described in the following paragraphs.

Before the beginning of cracking, beam is find in linear elastic regime, then the deformations in the strengthening and the reinforcement develop identically and no difference is detected among behaviors of beams of group B and C.

With the appearing of the first crack in beam, is remarkable the difference between behavior of beams of group B and C. While for beams of group B, the deformations of strengthening (due to cracking) are more evident than the reinforcement; for beams of group C the reinforcement and strengthening possess similar deformations. This shows that the presence of steel fibers prevent the concentration of stress in the strengthening due to propagation of cracks, in this case, in the midspan.

Regarding Figure [12-d], can be observed that the yield of reinforcement is proceeded by a defined platform of deformations. This behavior is characteristic of steel bars of class A and is different from the observed in the other beams. This fact occurred due to incautiousness in confection of beams reinforcement. However, in nothing harmed the analysis of results. A comparison between values of specific deformation of strengthening in the shearing midspan (strain gauge 3) and in the free midspan (strain gauge 1) of beams of group B and C is made in Figure [13].

In the midspan, considering a same level of load applied to beams, the Figure [13-a] shows that the cracking increased abruptly the strengthening deformation of molded beams with common concrete, while the presence of steel fibers in beams VR2-1 and VR2-2 decreased the strengthening deformations.

In the shearing midspan the strengthening deformations of beams of group C also reached higher values than the beams strengthening of group B (Figure [13-b]).

5. Numerical model

In this item is described the analysis of finite elements developed with the purpose to compare the obtained results to the experimental, basing still more these last. The non-linear numerical analysis of strengthened beams and without strengthening was lead using the Diana program version 9.1, based on the finite elements method (MEF). In Figure 14 are presented the mesh of finite elements and the geometric disposal of reinforcements defined in the program.

The boundary conditions were established so as to represent the test conducted in laboratory. The mesh of finite elements was elaborated using quadratic elements of eight knots of the type CQ16M with uniform dimensions. For discrete reinforcements were used elements of the type “embedded reinforcement”.

The knots of the external strengthening elements (Figure 14) were connected to adjacent knots of the elements of concrete simulating a perfect adherence between materials.

The models of finite elements were loaded by the imposition of a concentrated force of the type *“displace”*. This option allowed to load the model in similar way which were conducted the tests, that is, by displacement control.

The inferior and superior steel bars of beams reinforcement were modeled considering the strain-hardening observed in the conducted tests of characterization. The values of stress and plastic deformations of the reinforcement defined in the Diana program are illustrated in Figure 15-a. The direct tensile strength of the concrete was taken according to ACI-318M [11] as $0{,}332 \cdot \sqrt{f_c}$. For the cement composite the strength to direct tensile was taken according to RILEM [8] as $0{,}6 \cdot f_{fct,L}$. The post-peak behavior was represented with the *“Exponential softening in stress”*, considering for that purpose the energy of fracture calculated until one δ = 2, 65 mm with basis on the curves P-δ of flexural test in three points conducted (Figure 15-b).

In Figure 16 is presented the evolution of vertical displacements of a knot situated underside the beam, in the same line of application

Figure 14 – Numerical model

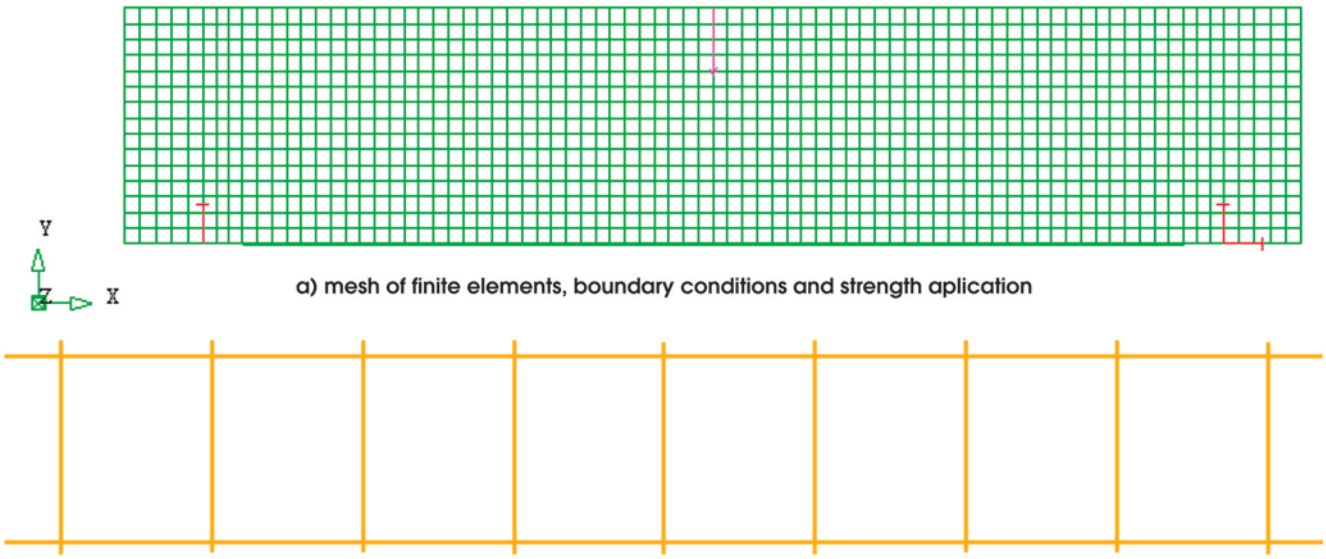

a) mesh of finite elements, boundary conditions and strength aplication

b) inferior reinforcement, superior and stirrups

of the concentrated load. These displacements are compared with the experimentally obtained.

Considering only the elastic phase of the beams behavior, it can be affirmed that the numerical and experimental curves are identical. However, after the concrete cracking differences are noticed in the curves behavior, since for the strengthened beams the numerical curves presented more stiffness than the experimental.

After the reinforcement yield, the numerical curve of beam without strengthening showed to have an intermediate behavior, between the two experimental curves of the beams VRE-1 e VRE-2. However, is observed that the first crack in the concrete occurred for a value of experimental load expressively lower than the numerically obtained. Such fact can be associated with the concrete strength to direct tensile.

After the first crack and even before the reinforcement yield, is observed an accented debonding of experimental curves in relation to numerical. From the experimental curve, is observed that the applied load to beams decreases in function of the stiffness loss provoked by concrete cracking. This effect was not represented in the numerical curve. The curves return to approximate, practically in the load level referent to the reinforcement yieldning, maintaining a satisfactory similarity until the test conclusion.

Figure 15 – Parameters for reinforcement and cimentitious composite

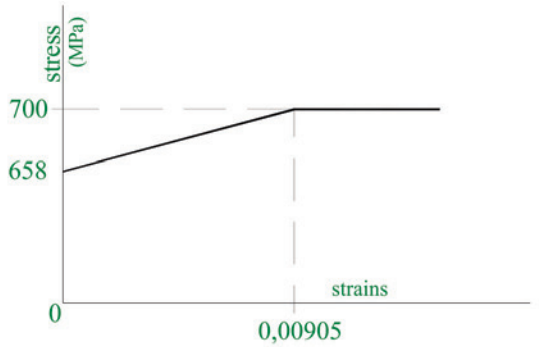

a) reinforcement plastic stress-strain

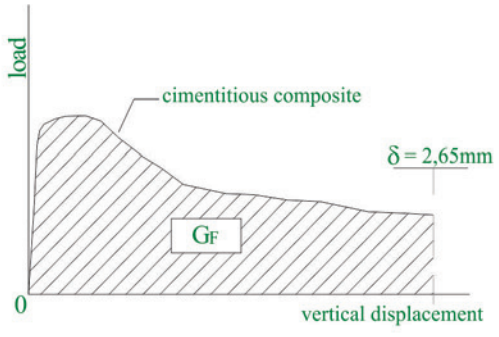

b) cimentitious composite strength-displacement

Figure 16 – Numerical and experimental vertical displacements

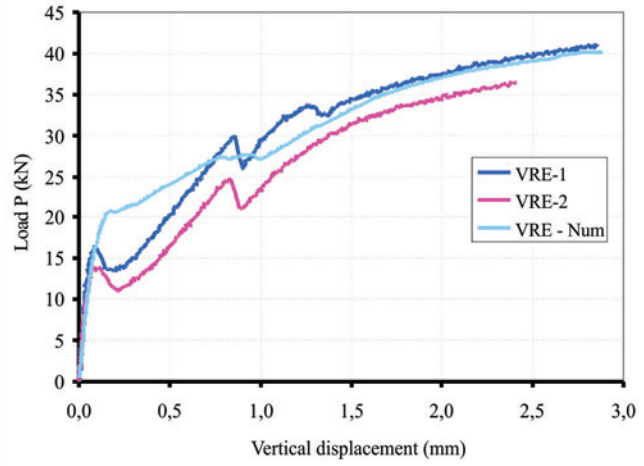

a) Beam VRE – group A

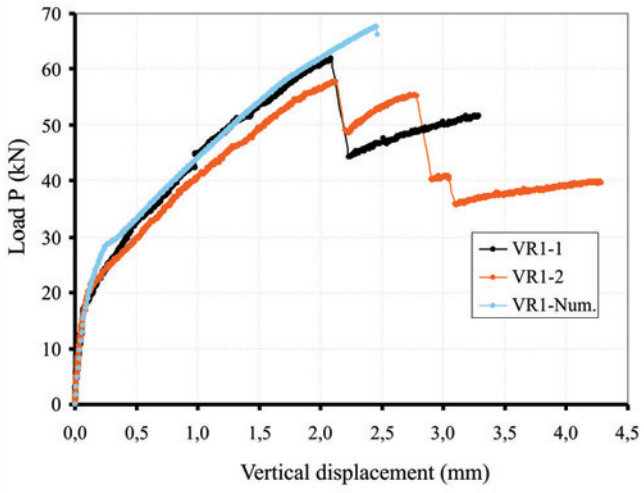

b) Beam VR1 group B

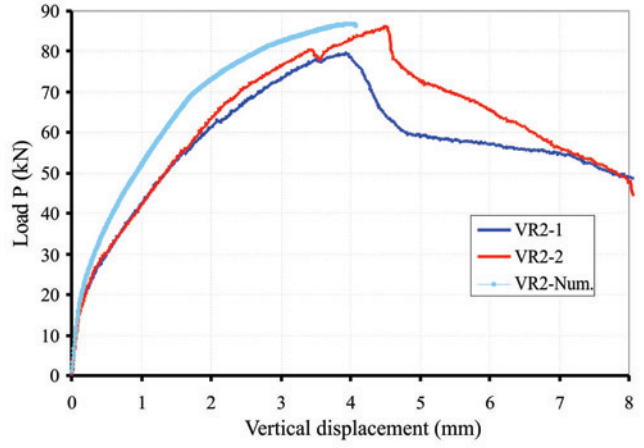

c) Beam VR2 – group C

The representative numerical curve of the beams behavior of group B presented satisfactory conformity with the experimental, especially with the VR1-1 beam. It is observed that after the concrete cracking the numerical curve showed higher stiffness than the curve VR1-2 and with a very similar evolution to VR1-1 beam.
The ultimate numerical load is 13, 0% superior to the average value experimentally obtained. The arrows corresponding to the ultimate loads of beams VR1-1 and VR2-1 were respectively, 2,09 mm and 2,12 mm, whereas the obtained via MEF was 2,46 mm, that is, 16, 6% superior to the average experimentally registered.
The fact of the non-linear analysis conducted with the Diana computational program has not taken account of the stiffness loss effect due to the unfastening process of the strengthening, as well as the idealization of perfect adherence between steel bars and the concrete, explain the surpass of the experimental loads values by numerical and also the higher stiffness of numerical curve.
The numerical curve of beams of group C showed also higher stiffness than the experimental curves. The rupture load obtained via MEF is 4, 6% higher than the average load experimentally obtained. The ultimate arrow of the numerical curve was 4, 08 mm, while the experimental was 3, 93 mm and 4, 50 mm.
However, is correct to affirm that despite the relative homogeneity of the numerical model when compared with the heterogeneity of analyzed beams in the laboratory and the considered simplifications in the model (principally the direct tensile strength of the cement composite and the use of the G_F to define its post-peak behavior), the numerical results could be able to represent satisfactorily the experimental behavior of beams of group C.
The Figure 17 compares the evolution of numerical and experimental deformations of strengthening in the free midspan of beams. It is observed that the strengthening deformations obtained via MEF and the experimental are similar, principally for beams of group C. In this case, the maximum deformation obtained numerically was 8, 40‰, while the experimental was 6, 96‰ and 8, 38‰.
For the beams of group B, the maximum experimental deformations of strengthening were 4,82‰ and 5,05‰. While the maximum numerical deformation of strengthening was 5, 19‰, that is only 5, 1% superior to the experimental average.
After the concrete cracking and considering even the same load value, the strengthening deformations via MEF showed much lower than the experimental. The concrete cracking provokes concentration of stress in the strengthening (as already seen). However, this effect was not reproduced in the numerical model. Moreover, is interesting to note that for beams of group C, as the steel fibers prevent the concentration of stress on the strengthening, the numerical curve better approximated to the experimental (as already seen).

6. Conclusions

In synthesis, from an experimental study and a numerical simulation by finites elements, the principal conclusions are:

- The use of a mortar-cement composite which contains short steel fibers modified the mode of failure of strengthened beams to flexural efforts;
- The fragile mode of failure, without warning, by unfastening of the strengthening due to the appearance of a crack in the shearing midspan was prevented, when a cement composite was used;

Figure 17 – Numerical and experimental strains of strengthening in the midspan

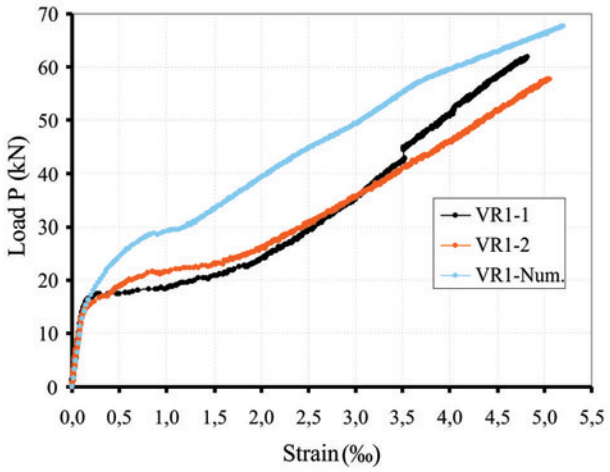

a) beam VR1

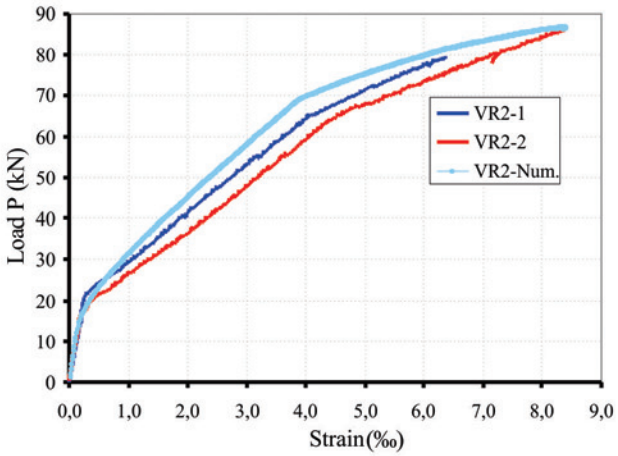

b) beam VR2

- The presence of short steel fibers enhanced considerably the post-cracking behavior of the strengthened beam, since, the fragile rupture was modified to a more ductile rupture with gradual loss of strength of the piece;
- A higher strengthening deformation of molded beams with the cement composite was reached;
- The action mechanism of the short steel fibers demonstrated to be possible to prevent the stress concentration in the strengthening, to alter the cracks aspect along the strengthening extent and even to turn the rupture more ductile, which until the moment was considered premature and fragile;
- The numerical simulation, using the Diana computational program, satisfactorily reproduced the experimental results. The arrow values, deformations and stress, were obtained as in the linear phase as in the non-linear, approximated to the experimental;
- In the general, the numerical curves of strengthened beams demonstrated to have more stiffness than the experimental. The fact is related to not taken account the reduction of beam stiffness due to the strengthening debonding;
- The use of fracture energy of the cement composite as a parameter to characterize its post-cracking behavior, showed to be possible to represent satisfactorily the strengths and experimental deformations values.

6. Acknowledgements

The author acknowledge FAPESP (Fundação de Amparo à Pesquisa do Estado de São Paulo) for finantial support during the doctoral studies and Maccaferri – América Latina by donation of steel fibers.

7. References

[01] FERRARI, V.J. Reforço à flexão de vigas de concreto armado com manta de polímero reforçado com fibras de carbono (PRFC) aderido a substrato de transição constituído por compósito cimentício de alto desempenho, São Carlos, 2007, Tese (doutorado) – Escola de Engenharia de São Carlos, Universidade de São Paulo, 322 p.

[02] BUYUKOZTURK, O.; KARACA, E. (2004). Progress on understanding debonding problems in reinforced concrete and steel members strengthened using FRP composites. Construction and Building Materials, 24, p. 9-19.

[03] WU, Z.S.;YIN, J. (2003). Structural performances of short steel-fiber reinforced concrete beams with externally bonded FRP sheets. Construction and Building Materials, 17, p.463-470.

[04] CARRAZEDO, R. (2005). Mecanismos de confinamento em pilares de concreto encamisados com polímeros reforçados com fibras submetidos à flexo-compressão. 267p. Tese (Doutorado) – Universidade de São Paulo, Escola de Engenharia de São Carlos, São Carlos, 2005.

[05] ASSOCIAÇÃO BRASILEIRA DE NORMAS TÉCNICAS. Concreto – Ensaio de compressão de corpos-de-prova cilíndricos – NBR 5739. Rio de Janeiro, 1994.

[06] ASSOCIAÇÃO BRASILEIRA DE NORMAS TÉCNICAS. Argamassa e concreto – Determinação da resistência à tração por compressão diametral de corpos-de-prova cilíndricos – NBR 7222. Rio de Janeiro, 1994.

[07] ASSOCIAÇÃO BRASILEIRA DE NORMAS TÉCNICAS. Materiais metálicos – Determinação das propriedades mecânicas à tração – NBRISO 6892. Rio de Janeiro, 2002.

[08] RILEM TC 162-TDF. Test and design methods

for steel fibre reinforced concrete, Materials and Structures, v.35, p. 579-582, 2002.

[09] RILEM (1985). Draft Recommendation, 50-FMC Committee Fractures Mechanics of Concrete. Determination of fracture energy of mortar and concrete by means of three-poin bend tests on notched beams. Materials and Structures/Matériaux et Constructions, v.18, n.106, p. 285-290.

[10] FEDERATION INTERNATIONALE DE BETON – FIB (1999). Structural concrete textbook on behavior design and performance. Updated knowledge of the CEB/FIP Model Code 1990, v.1. International Federation for Structural Concrete (FIB), Switzerland.

[11] AMERICAN CONCRETE INSTITUTE. ACI 318M: Building code requirements for reinforced concrete. Detroit.